

Modeling of Industrial High Pressure Autoclave Polyethylene Reactor Including Decomposition Phenomena

Hee-Jong Lee, Yeong-Koo Yeo[†] and Jin Yang Chang*

Department of Chemical Engineering, Hanyang University, 17 Haengdang-dong, Sungdong-ku, Seoul 133-791, Korea

*Daelim Industrial Co., Chung-Ku, Seoul, Korea

(Received 6 November 1999 • accepted 26 December 1999)

Abstract—The aim of the present work is the development of a practical model for an industrial high-pressure polyethylene plant. The reactor considered in this work is the adiabatic slim type autoclave with four zones for free radical polymerization of ethylene. A fairly comprehensive but realistic model is described that has the ability to predict the temperature at each reaction zone as well as the effects of initiator flow changes. From the stability analysis we could identify the range of operating conditions which can effectively be used to prevent decomposition phenomena (runaway reactions) and to maximize polymer conversion in LDPE autoclaves.

Key words: LDPE, Autoclave Polyethylene Reactor, Decomposition Reactions Runaway Phenomena, Free Radical Polymerization

INTRODUCTION

Free radical polymerization of ethylene at high pressure has been used in the polymer industry for years to produce low-density polyethylene (LDPE). Although transition metal-catalyzed low-pressure ethylene polymerization processes (gas-phase and slurry-phase Ziegler-Natta processes) have gained popularity in the polyolefin industry in recent years, a significant amount of low-density polyethylene is still manufactured world-wide by high-pressure free radical polymerization processes. Moreover, some applications of high-activity transition metal catalysts to high-pressure reactor systems and the use of conventional high-pressure polyethylene reactors to produce copolymers have recently been reported and we can see that high-pressure polymerization technology will likely remain quite competitive in the future.

High-pressure polyethylene processes are characterized by high-reaction temperature (150-300 °C) and pressure (1,000-3,000 atm). Two types of processes are commonly used: a tubular process using a very long, small-diameter tubular reactor and an autoclave process using a well-stirred tank reactor. It is well known that polyethylene products manufactured by these processes differ in their molecular architecture and in their end use properties. The two processes enjoy equal popularity in industrial practice. Decomposition reactions occur less frequently in tubular processes due to a higher cooling surface area than in the autoclave reactor.

Since decomposition reactions occur over a very small time interval [Huffman et al., 1974] there is no practical way to control the high temperature and pressure in the reactor once the decomposition reactions have started. Thus, it is common for LDPE reactors to be equipped with relief valves that open at a specified upper pressure limit.

Many results can be found on modeling LDPE autoclave and

tubular reactors [Agrawal and Han, 1975; Ahn et al., 1985; Brandolin et al., 1988; Chan et al., 1993; Chen et al., 1976; Feucht et al., 1985; Goto et al., 1981; Han and Liu, 1977; Hollar and Ehrlich, 1983; Marini and Georgakis, 1984; Mavridis and Kiparissides, 1985; Shirodkar and Tsien, 1986; Yoon and Rhee, 1985; Zabisky et al., 1992]. But most of these results deal with only polymerization and polymer molecular structure due to the lack of a fundamental understanding of the decomposition reactions. Descriptions of typical decomposition phenomena can be found elsewhere [Zhang et al., 1996]. The purpose of the present study is to identify the range of operating conditions to prevent decomposition reactions based on the plant model. We developed a steady-state model of an actual autoclave reactor based on combined polymerization [Ham and Rhee, 1996; Lee et al., 1999] on the assumption of perfect mixing. Decomposition phenomena due to excess initiator flow, excess monomer flow and excess initiator concentration were also investigated.

POLYMERIZATION KINETICS

A deterministic description of the free radical polymerization reaction mechanism is well established [Ehrlich and Mortimen, 1971] and is summarized in Table 1. This reaction scheme can be extended by including various chain-transfer reactions to account for branching reactions that affect many important polymer properties. The primary objective of the present work is to analyze overall reactor behaviors and to evaluate effects of key variables (initiator flow, monomer flow and initiator concentration) to identify operating conditions causing decomposition phenomena.

Ethylene and polyethylene may exist as a single phase or two phases at normal operating temperature and pressure. In case of two phases, the frequency of long-chain branching decreases on account of diminution of transferring property of polymer-chain [Solvik and Kinch, 1983]. To consider this trend, we used a kinetic constant with long chain branching functional relation of given

[†]To whom correspondence should be addressed.

E-mail: ykyeo@email.hanyang.ac.kr

Table 1. Free radical polymerization mechanism

Initiation	$I_2 \xrightarrow{k_2} 2\phi$
	$\phi + M \xrightarrow{k_3} R_1$
Propagation	$R_1 + M \xrightarrow{k_4} R_2$
	$R_2 + M \xrightarrow{k_4} R_{j+1}$
Termination by combination	$R_j + R_j \xrightarrow{k_5} R_{j+j}$
Termination by disproportionation	$R_j + R_i \xrightarrow{k_6} P_j + P_i$
Chain transfer to monomer	$R_j + M \xrightarrow{k_7} P_j + P_i$
Chain transfer to polymer	$R_j + P_i \xrightarrow{k_8} P_j + R_i$
Back biting	$R_j \xrightarrow{k_9} R_j$

temperature and pressure.

The symbols I , ϕ , M , R , and P , represent the initiator, free radical, monomer, living polymer, and dead polymer, respectively. The reaction constants except k_p are assumed to be independent of the chain length j and hence can be determined at any temperature and pressure by the Arrhenius relation. The rate constant for the chain transfer to the polymer is considered to take the form of $j k_p$ [Ham et al., 1996].

KINETICS OF DECOMPOSITION

The rapid decomposition of ethylene brings about runaway phenomena. Many researchers attempted to identify decomposition kinetics and kinetic rate constants [Hucknall, 1985; Miller, 1969; Tarzawa and Gardiner 1980]. So far reliable results on the decomposition kinetics have not yet been presented. Zhang et al. [1996] analyzed the runaway phenomena based on Watanabe's mechanism kinetics based on the scheme originally proposed by Watanabe et al. [1972] as shown in Table 2. Simplified expressions for the decomposition elements can be given by

$$\frac{d[C]}{dt} = k_3[C_2H_3] = \frac{k_6}{2\sqrt{k_1}} [M]^2 \quad (1)$$

$$\frac{d[CH_4]}{dt} = k_5[M][CH_3] + k_8[C_2H_3][CH_3] = \left(\frac{k_1}{2} + \frac{k_6}{2\sqrt{k_1}}\right) [M]^2 \quad (2)$$

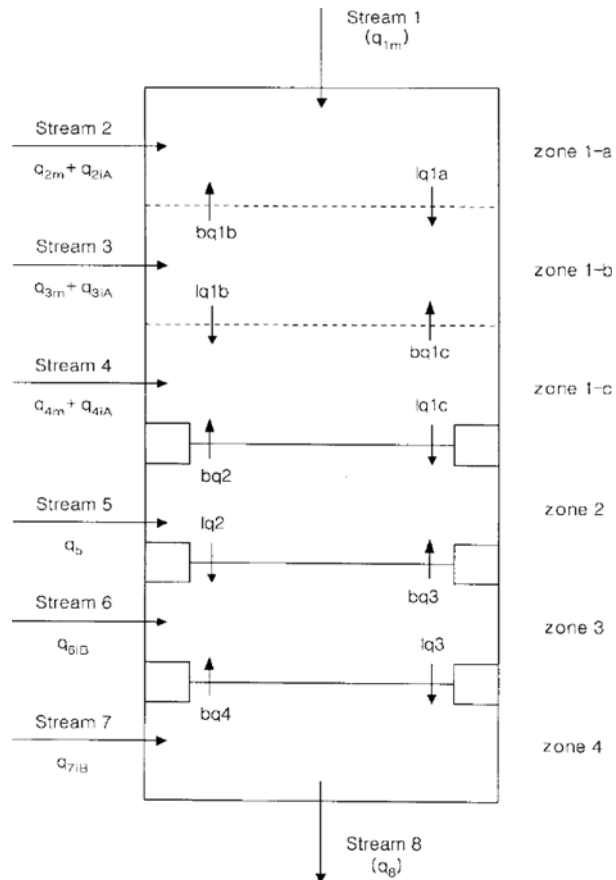
$$\frac{d[C_2H_6]}{dt} = k_3[M][C_2H_5] + k_7[CH_3]^2 = \frac{3}{2}k_1[M]^2 \quad (3)$$

$$\frac{d[C_2H_2]}{dt} = k_3[C_2H_3][CH_3] + k_9[C_2H_3]^2 = k_1[M]^2 \quad (4)$$

With the simplified decomposition scheme, there are only two independent rate constants that need to be determined: k_1 and $k_6k_3^{0.5}$. They can be determined from two pieces of information:

Table 2. Ethylene decomposition mechanism

Initiation	$2C_2H_4 \xrightarrow{k_1} C_2H_3 + C_2H_5$
Propagation	$C_2H_5 \xrightleftharpoons{k_2, k_3} C_2H_4 + H$
	$C_2H_5 + C_2H_4 \xrightarrow{k_4} C_2H_6 + C_2H_3$
	$H + C_2H_4 \xrightarrow{k_5} H_2 + C_2H_3$
	$C_2H_3 \xrightarrow{k_6} C + CH_3$
	$CH_3 + C_2H_4 \xrightarrow{k_7} CH_4 + C_2H_3$
Termination	$CH_3 + CH_3 \xrightarrow{k_8} C_2H_6$
	$C_2H_3 + CH_3 \xrightarrow{k_9} C_2H_2 + CH_4$
	$C_2H_3 + C_2H_3 \xrightarrow{k_10} C_2H_2 + C_2H_4$

**Fig. 1. Schematic diagram of reactor.**

the crossing temperature of the decomposition reaction rate with the polymerization rate and the decomposition products distribution at a specified temperature [Zhang et al., 1996].

MASS AND ENERGY BALANCES

The industrial reactor being modeled is an adiabatic slim-type autoclave reactor with four reaction zones as shown in Fig. 1. We divided the first zone into three cells, since its volume is much larger than that of the other zones and monomers are fed into three different locations in the zone. Certain degree of back flow is assumed to incorporate mixing effects. Operational data on volumes and temperatures at each reaction zone and inlet streams used in the simulations are shown in Tables 3 and 4.

1. Mass Balance

The mass balances can be written as

$$V_i \frac{dC_j}{dt} = Q_{input}C_{input,j} - Q_{output}C_{j,i} + V_i t C_j \quad (5)$$

$$\left(\begin{array}{l} j=I, M, G, G', G'', F, F', F'', C, CH_4, C_2H_6, C_2H_2 \\ i=zone 1, 1b, 1c, 2, 3, 4 \end{array} \right)$$

The first subscripts in C_j represent the quantities in the order of I , M , G , G' , G'' , F , F' , F'' , and decomposition products (C , CH_4 , C_2H_6 , C_2H_2). I and M are the concentrations of initiator and monomer, G and F are the total concentrations of living and dead

Table 3. Inlet streams to reactor

Zone		Feed property	Volume flow (l/min)	Concentration (gmol/l)	Feed temp. (°C/K)	Remarks
Zone 1	Zone 1-a	Q_{1m}	Monomer	717	15.27	35/308
		q_{2m}	Monomer	717	15.27	35/308
		q_{3IA}	Initiator A	600	1.84×10^{-3}	35/308
	Zone 1-b	q_{3m}	Monomer	717	15.27	30/303
		q_{3IA}	Initiator A	189.42	1.83×10^{-3}	30/303
	Zone 1-c	q_{4m}	Monomer	717	15.27	30/303
		q_{4IA}	Initiator A	134.4	1.83×10^{-3}	30/303
Zone 2		q_5	cat-solvent		40/313	not concerned
Zone 3		q_{6B}	Initiator B	10.5	5.4×10^{-3}	40/313
Zone 4		q_{7B}	Initiator B	10.5	5.4×10^{-3}	40/313

Table 4. Reactor volume and temperature (pressure P=1,335 atm)

Reactor zone	Volume		Temperature (steady-state)	
	Symbol	Value (litter)	Symbol	Value (k)
1-a	V_{1a}	220	T_{1a}	498
1-b	V_{1b}	220	T_{1b}	493
1-c	V_{1c}	440	T_{1c}	493
2	V_2	220	T_2	498
3	V_3	220	T_3	533
4	V_4	310	T_4	568

Table 5. The expressions for r_g

$$\begin{aligned}
 r_i &= -k_d I \\
 r_M &= -2fk_d I - k_p MG - k_{im} MG \\
 r_G &= 2fk_d I - (k_{ic} + k_{id})G^2 \\
 r_{G'} &= 2fk_d I + k_p MG - (k_{ic} + k_{id})GG' + k_{im} M(G - G') + k_{ip}(GF'' - G'F') \\
 r_{G''} &= 2fk_d I + k_p M(2G' + G) - (k_{ic} + k_{id})GG'' + k_{im} M(G - G'') \\
 &\quad + k_{ip}(GF'' - G'F') \\
 r_p &= k_d G^2 + (k_{ic}/2)G^2 + k_{im} MG \\
 r_{p'} &= (k_{ic} + k_{id})GG' + k_{im} MG' + k_{ip}(G'F' - GF'') \\
 r_{p''} &= k_{id} GG'' + k_{ic}(GG'' + G'^2) + k_{im} MG'' + k_{ip}(G''F' - GF'')
 \end{aligned}$$

polymers, and the prime and double prime are the concentrations of first and second moments, respectively. The second subscript i indicates the cell number. The rate of backflow between the zones is specified by comparing the simulation results with the plant data. The expressions for r_g are given in Table 5. In the simulations pseudo steady-state was assumed and the closure technique of Hulbert and Katz [1964] was used to obtain F'' .

The initiators being used in the plant and considered in the present study are di-t-butyl peroxide (initiator type A) and t-butyl-peroxy 2-ethyl-bexapate (initiator type B). The parameters for the reaction rate constants are taken from elsewhere [Ham and Rhee, 1996] with little adjustments and summarized in Table 6. The initiator decomposition efficiency f is 0.3 for initiator type A and 0.2 for initiator type B.

2. Energy Balance

Density for the single-phase reaction mixture can be given by [Benzler and Koch, 1955]

Table 6. Kinetic constants

Reaction	k_0 [l/(mol·s) or s^{-1}]	E_a [cal/mol]	V_a^{**} [cal/(atm·mol)]
Polymerization	Ak_d	1.309×10^{19}	33872
	Bk_d	1.396×10^{13}	30103
	k_p	4.16×10^6	6477-0.56P
	k_{ic}	3×10^8	3950
	k_{id}	3×10^8	3950
	k_{im}	1.9×10^6	11778-0.48P
Decomposition	k_p	3×10^4	9375-0.48P
	k_i	4.003×10^{19}	65000
	$k_d k_i^{-0.5}$	1.587×10^{20}	65000
	ΔH_{poly}	21400 cal/mol	
	ΔH_{decomp}	30200 cal/mol	

* $k_i = k_{i0} \exp[-(E_i/RT)]$: Arrhenius equation used for polymerization

* $k_d = k_{d0} \exp[-(E_d + V_a P)/RT]$: Arrhenius equation used for decomposition

$$\begin{aligned}
 P &= 1995.85 - 601.2 \log_{10}\left(\frac{P}{1000}\right) + 593.3 \log_{10}\left(\frac{1}{T}\right) \\
 &\quad - 335.8 \log_{10}\left(\frac{P}{1000}\right) \log_{10}\left(\frac{1}{T}\right)
 \end{aligned} \quad (6)$$

Heat capacity (C_p) is assumed to be constant as 0.583 cal/g·K [Michels and DeGroot, 1946]. Energy balance at each zone is given by

$$\begin{aligned}
 \rho_i C_p V_i \frac{dT_i}{dt} &= \rho_i C_p [Q_{input} T_{input} - Q_{output} T_i] \\
 &\quad + V_i [r_p (-\Delta H_{poly}) + r_d (-\Delta H_{decomp})] + V_i P_i
 \end{aligned} \quad (7)$$

($i = \text{zone 1a, 1b, 1c, 2, 3, 4$)

where T denotes the reaction temperature, r_p is the polymerization rate, r_d is the decomposition rate and P_i represents the rate of heat generation per unit volume by agitation. P_i can be obtained from

$$P_i = 1.37 f_{\mu} \rho n^2 d^5 \quad (8)$$

where ρ , n , d , and f_{μ} represent the density, the agitation speed, the impeller diameter and the viscosity correction factor, respectively. With an agitation speed of 720 rpm the value of P_i remains constant at 15.02 cal/s·l.

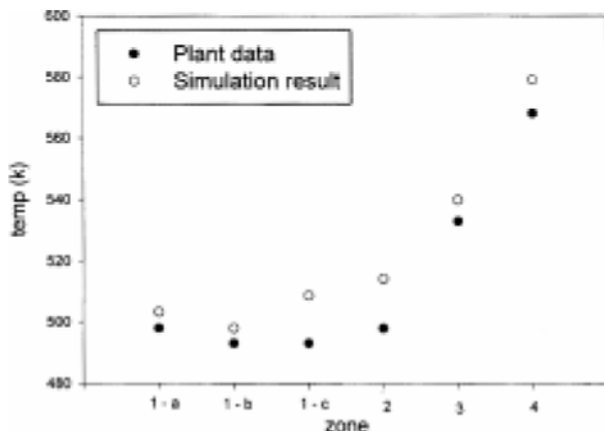


Fig. 2. Temperature profile of simulation results and plant data on each zone.

RESULTS AND DISCUSSION

Continuation analysis of the reactor offers important information regarding possible steady states and their stability. Many results were published on continuation analysis of the LDPE autoclave [Gardner 1975; Hoftyzer and Zwietering, 1961]. However, all of those results considered only polymerization mechanisms in their models, which significantly limited the predictive power of their reaction models. In this study, we put emphasis on suggesting operation limits for three variables (initiator flow rate, monomer flow rate and initiator concentration in feed) to prevent runaway phenomena based on the model including both polymerization and decomposition kinetics. The steady-state model of the actual reactor was developed first and continuation analyses were performed on the three variables mentioned above.

Fig. 2 shows the results of simulations and plant data on ordinary operating conditions. A little discrepancy can be seen between simulation results and plant data, but the model shows a changing trend similar to that observed in the plant.

1. Effects of Initiator Flow Rates

Initiators are injected to the reactor through five stream lines: q_{2A} , q_{3A} , q_{4A} , q_{5A} and q_{6A} . The locations of each stream line are as shown in Fig. 1. Figs. 3 and 4 show the effects of initiator flow on the conversion and temperature. Effects of variations of q_{2A} are shown in Fig. 3, and those of q_{4A} in Fig. 4, respectively. Effects of q_{3A} and q_{5A} show similar behavior to q_{2A} and q_{6A} , respectively. Onset of decomposition is characterized by sharp decrease of polymerization extent and reaction temperature (Fig. 3). But increase of q_{4A} rate does not cause decomposition as can be seen in Fig. 4. Figs. 3 and 4 clearly show the permissible operating range of initiator flow rates in order to prevent decomposition reactions.

2. Effects of Monomer Flow Rates

Monomers are fed into the zone 1-a, 1-b and 1-c as shown in Fig. 1. Effects of variations of each monomer stream q_{1m} and q_{2m} are shown in Figs. 5 and 6. Variations in q_{1m} and q_{2m} show similar behavior. In fact, the reaction temperature can be lowered by decreasing flow rates of q_{1m} and q_{2m} . In contrast to q_{1m} and q_{2m} , variations of q_{3m} and q_{4m} show quite different characteristics from q_{1m} and q_{2m} as can be seen in Fig. 6. From this fact we can see that

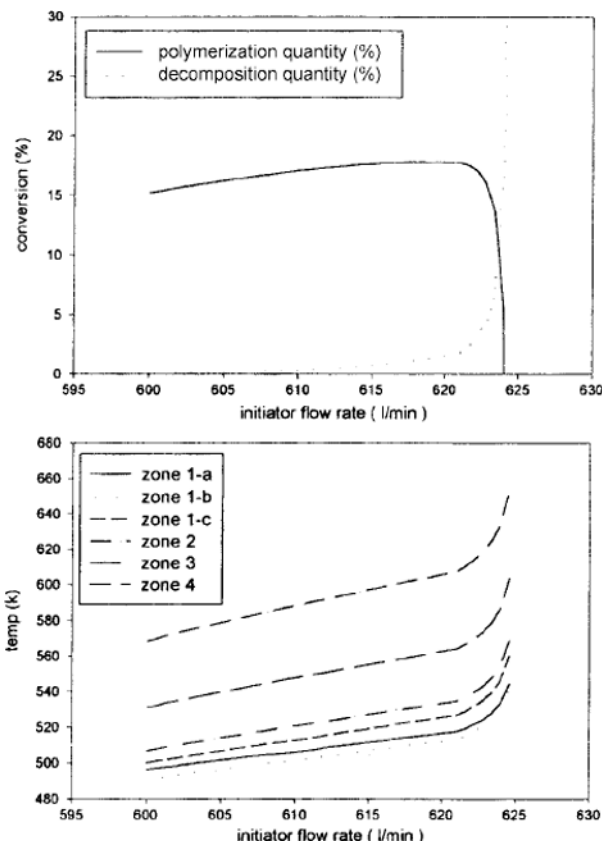


Fig. 3. Effects of q_{2A} on conversion and temperature.

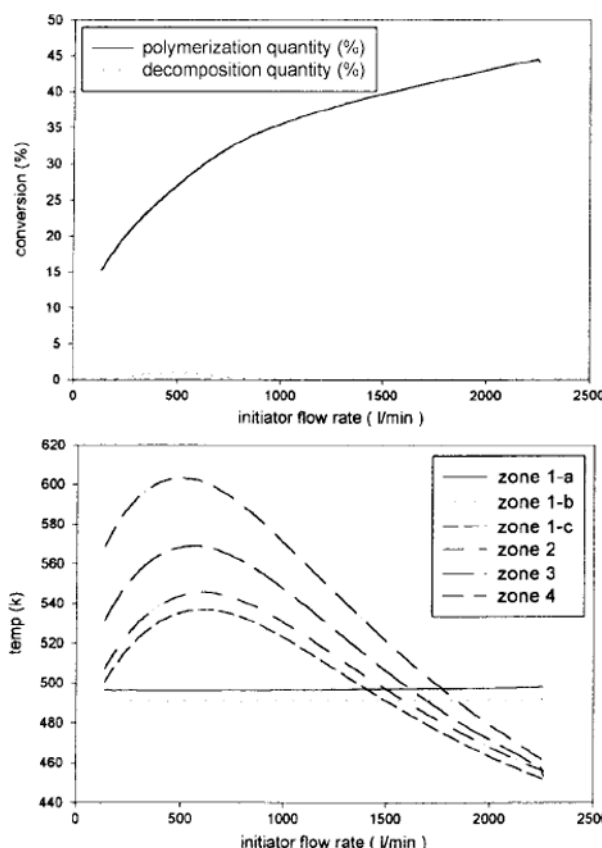
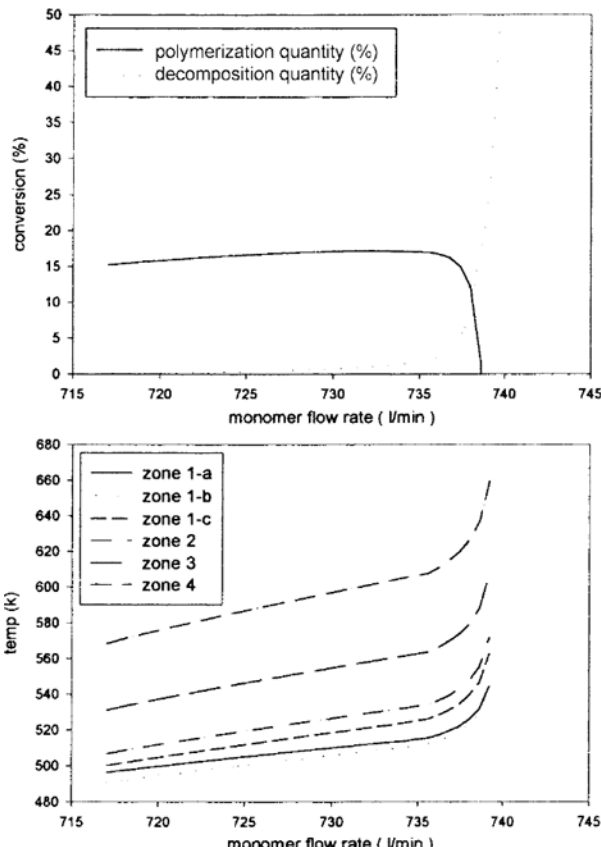
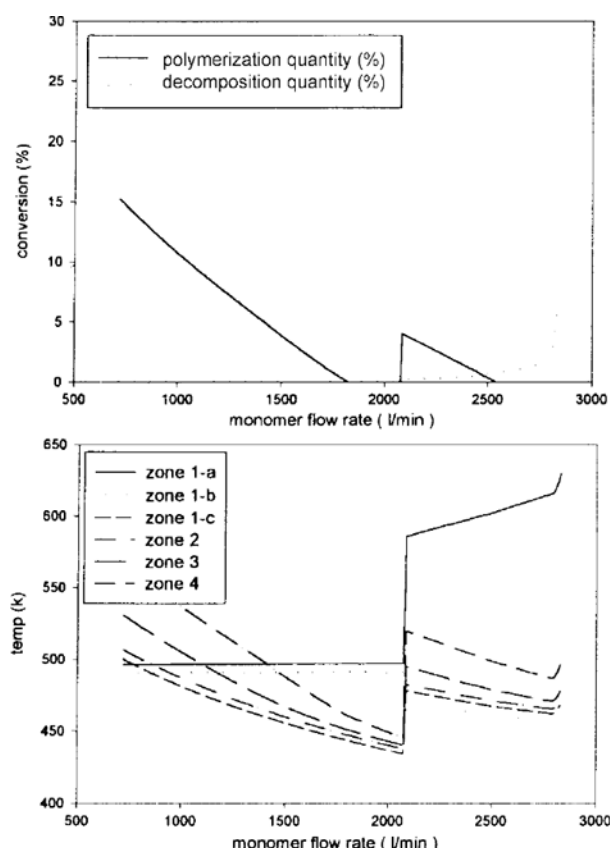
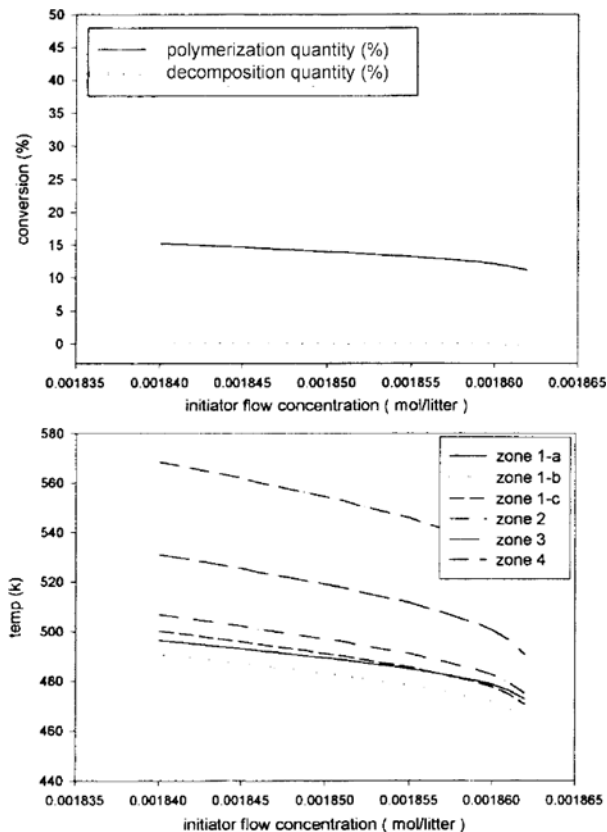


Fig. 4. Effects of q_{4A} on conversion and temperature.

Fig. 5. Effects of q_{2m} on conversion and temperature.Fig. 6. Effects of q_{4m} on conversion and temperature.Fig. 7. Effects of q_{244} concentration on conversion and temperature.

polymerization mainly occurs in reaction zone 1-a and q_{2m} and q_{4m} can be effectively used to control the reaction temperature. The threshold in the monomer flow rates which causes decomposition reactions can easily be identified from Figs. 5 and 6.

3. Effects of Initiator Concentrations

Figs. 7 and 8 show the effects of variations in initiator concentrations on conversion and temperature. As can be seen in Fig. 7, increase of concentrations of q_{244} and q_{444} causes decrease in conversion and temperature and does not cause decomposition reactions. But certain values of q_{244} and q_{444} concentrations cause decomposition phenomena. Effects of variations in q_{144} concentration show similar behavior with those of q_{244} . Unconditional increase of initiator concentrations may deteriorate the polymerization process as can be seen in Figs. 7 and 8.

CONCLUSIONS

A practical model for an industrial high-pressure polyethylene plant was developed. The slim type autoclave reactor was divided into four reaction zones and combined polymerization was employed in the modeling. In order to identify permissible operating range to prevent decomposition reactions, effects of variations in the initiator and monomer flows were examined. From the simulations we could easily identify the threshold of runaway phenomena. Results of the present study can be effectively used in the operation to increase conversion while avoiding decomposition reactions.

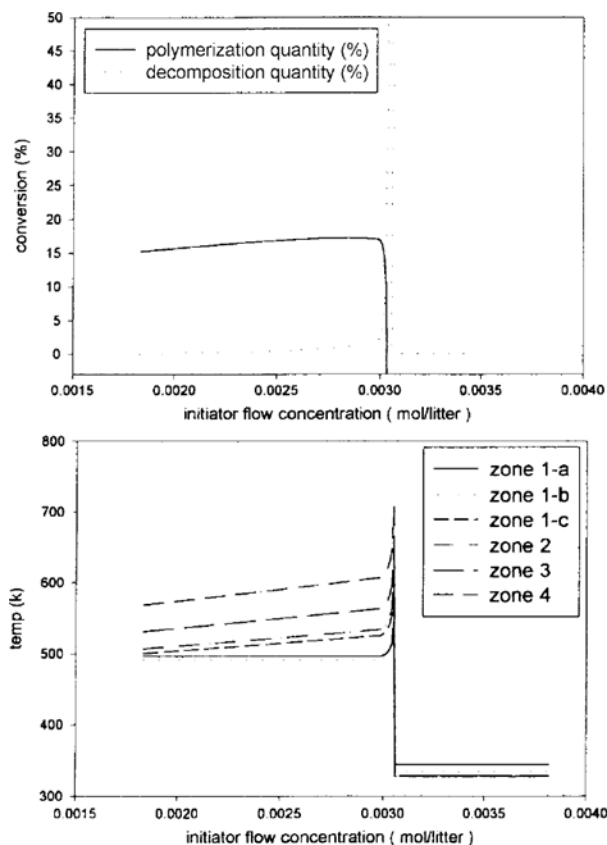


Fig. 8. Effects of q_{44} concentration on conversion and temperature.

NOMENCLATURE

$C_{input,j}$: concentration of species j in the inlet volumetric flow rate [mol/l]
C_p	: concentration of species j in the zone i [mol/l]
C_p	: heat capacity [cal/(g·K)]
d	: impeller diameter
E_a	: activation energy of the Arrhenius equation [cal/mol]
F	: concentration of dead polymer [mol/l]
f	: initiator decomposition efficiency
G	: concentration of living polymer [mol/l]
I	: concentration of initiator [mol/l]
k	: reaction rate constant [s^{-1} for initiation, $l/(mol\cdot s)$ for the others]
M	: concentration of monomer [mol/l]
n	: agitation speed [s^{-1}]
P	: pressure [atm]
Q_{input}	: inlet volumetric flow rate [l/s]
Q_{output}	: outlet volumetric flow rate [l/s]
T_i	: temperature of the zone i [K]
T_{input}	: temperature of inlet volumetric flow rate [K]
t	: time [s]
V_i	: volume in the zone i [l]
f_μ	: viscosity correction factor
r	: reaction rate [mol/(l·sec)]

Greek Letters

March, 2000

ρ : density [g/l]
 ΔH_{decomp} : heat of ethylene decomposition (cal/mol)
 ΔH_{poly} : heat of polymerization (cal/mol)
 ϕ : concentration of free radical

REFERENCES

Agrawal, S. and Han, C. D., "Analysis of the High Pressure Polyethylene Tubular Reactor with Axial Mixing," *AICHE J.*, **21**, 449 (1975).

Ahn, Y. C., Rhee, H. K. and Choi, C. K., "Performance Analysis of a High Pressure Polyethylene Tubular Reactor," *HWAHAK KONGHAK*, **23**, 399 (1985).

Benzler, Von Dr.-Ing. H. and Koch, A. V., "Ein Zustandsdiagramm für Äthylen bis zu 10000 ata Druck," *Chemie-Ing. Techm.*, **27**, 71 (1955).

Brandolin, A., Capiati, J. N. F. N. J. and Vales, E. M., "Mathematical Model for High Pressure Tubular Reactor for Ethylene Polymerization," *Ind. Eng. Chem. Res.*, **27**, 784 (1988).

Chan, W. M., Gloor, P. E. and Hanielec, A. E., "A Kinetic Model for Olefin Polymerization in High Pressure Polyethylene Reactor," *AICHE J.*, **39**, 111 (1993).

Chen, C. H., Vermeychuk, J. G., Howell, J. A. and Ehrlich, P., "Computer Model for Tubular High Pressure Polyethylene Reactor," *AICHE J.*, **22**, 463 (1976).

Ehrlich, P. and Mortimer, G. A., "Fundamentals of the Free-radical Polymerization of Ethylene," *Adv. Polym. Sci.*, **7**, 336 (1971).

Feucht, P., Tilger, B. and Luft, G., "Prediction of Molar Mass Distribution, Number and Weight Average Degree of Polymerization and Branching of Low Density Polyethylene," *Chem Eng. Sci.*, **40**, 1935 (1985).

Gardner, G. M., "A Theoretical Study of the Kinetics of Polyethylene Reactor Decompositions," MS Thesis, Texas Tech Univ., Lubbock (1975).

Goto, S., Yamamoto, K., Furui, S. and Sugomoto, M., "Computer Model for Commercial High Pressure Polyethylene Reactor Based on Elementary Reaction Steps Obtained Experimentally," *J. Appl. Polym. Sci.*, **36**, 21 (1981).

Ham, J.-Y. and Rhee, H.-K., "Modeling and Control of an LDPE Autoclave Reactor," *J. Proc. Cont.*, **6**, 241 (1996).

Han, C. D. and Liu, T. J., "The Performance of High Pressure Polyethylene Tubular Reactor with Multiple Injections of Initiator and Monomer," *HWAHAK KONGHAK*, **15**, 249 (1977).

Hoffman, W. J., Bonner, D. C. and Gardner, G. M., "Decompositions in Polyethylene Reactors: A Theoretical Study," AICHE Meeting, Washington, DC, Paper 63d (1974).

Hoflyzer, P. J. and Zwietering, T. N., "The Characteristics of a Homogenized Reactor for the Polymerization of Ethylene," *Chem. Eng. Sci.*, **14**, 241 (1961).

Hollar, W. and Ehrlich, P., "An Improved Model for Temperature and Conversion Profiles in Tubular High Pressure Polymerization of Ethylene," *Chem. Eng. Sci.*, **14**, 241 (1961).

Hucknall, D. H., "Chemistry of Hydrocarbon Combustion," Chapman & Hall, London, 335 (1985).

Hulbert, H. M. and Katz, S., "Some Problems in Particle Technology," *Chem. Eng. Sci.*, **19**, 555 (1964).

Lee, J., Ham, J. Y., Chang, K. S., Kim, J. Y. and Rhee, H. K., "Anal-

ysis of an LDPE Compact Autoclave Reactor by Two-Cell Model with Backflow," *Polymer Eng. Sci.*, **39**, 1279 (1999).

Marini, L. and Georgakis, C., "Low Density Polyethylene Vessel Reactors Part I: Steady State and Dynamic Modeling," *AIChE J.*, **30**, 401 (1984a).

Marini, L. and Georgakis, C., "The Effect of Imperfect Mixing on Polymer Quality in Low Density Polyethylene Vessel Reactor," *Chem. Eng. Commun.*, **30**, 361 (1984b).

Mavridis, H. and Kiparissides, C., "Optimization of a High Pressure Polyethylene Tubular Reactor," *Poly. Process. Eng.*, **3**, 263 (1985).

Michels, A. and DeGroot, R. S., "ThermoDynamic Properties of Ethylene under Pressure up to 3000 Atmospheres and Temperatures between 0 °C and 150 °C, Tabulated as Functions of Density," *Physica*, **12**, 105 (1946).

Miller, S. A., "Biological Properties and Other Chemical Properties," *Ethylene and Its Industrial Derivatives*, S. A. Miller, ed., Ernest Benn, London, 1118 (1969).

Shirodkar, P. P. and Tsien, G. O., "A Mathematical Model for the Production of Low Density Polyethylene in a Tubular Reactor," *Chem. Eng. Sci.*, **41**, 1031 (1986).

Solvik, R. S. and Kinch, W., "The Development and Potential of the LDPE HP Autoclave Process," *Polyethylenes*, (1983).

Sullivan, J. F. and Shannon, D. I., "Decomposition Venting in a Polyethylene Product Separator," *Codes and Standards and Applications for High Pressure Equipment*, J. E. Staffiera, ed., ASME, New York, 191 (1992).

Tanazawa, T. and Gardiner, W. C., "Reaction Mechanism of the Homogeneous Thermal Decomposition of Acetylene," *J. Phys. Chem.*, **84**, 236 (1980).

Watanabe, H., Kurihara, K. and Takehisa, M., "The Explosive Decomposition of Ethylene," *Proc. Pacific Chemical Engineering Congress (PACHEC)*, AIChE, New York, 225 (1972).

Yoon, B. J. and Rhee, H. K., "A Study of the High Pressure Polyethylene Tubular Reactor," *Chem. Eng. Commun.*, **34**, 253 (1985).

Zabisky, R. C. M., Chan, W. M., Gloor, P. E. and Hamielec, A. E., "A Kinetic Model for Olefin Polymerization in High Pressure Tubular Reactors," *Polymer*, **33**, 2243 (1992).

Zhang, S. X., Read, N. K. and Ray, W. H., "Runaway Phenomena in Low-Density Polyethylene Autoclave Reactors," *AIChE J.*, **42**, 2911 (1996).